**Using PET/MRI to Assess Radioembolization of Y90 Microspheres**

**Target audience:** Body MRI radiologists, nuclear medicine physicians, interventional radiologists, radiation oncologists, interventional oncologists

**PURPOSE:** Radioembolization is used to treat cancer in the liver via intra-arterial delivery of yttrium-90 ($^{90}$Y) microspheres to the liver tumors. $^{90}$Y delivers high radiation dose to liver tumors with a risk of toxicity due to inadequate tumor coverage and extrahepatic deposition. There is a growing interest in post-delivery imaging of these $^{90}$Y microspheres to make assessments of possible extrahepatic deposition and toxicity as well as assessing tumor coverage to predict response. We tested the feasibility of using a hybrid PET/MRI scanner to assess distribution of $^{90}$Y microspheres and estimate dose received during treatment.

**METHODS:** Following IRB approval, we performed post-procedural imaging with a Siemens Biograph mMR scanner on 20 patients within 25 hours of $^{90}$Y delivery. MRI sequences included a 2 point DIXON sequence (TR = 3.6ms, TE1 = 2.46ms and TE2=1.23 ms, flip angle of 10 degrees) for attenuation correction of the PET images, diffusion weighted images (b values 50, 400, 800), and a 20 minute delayed post-contrast volumetric interpolated breath hold examination (VIBE) sequence in the axial and coronal planes. Intravenous contrast consisted with Gadoxetic acid (0.05 mmol/kg) administered at 1 ml/second. Regions of interest (ROIs) for the lesions, treated lobe, non-treated lobe, and normal were drawn on the 20 minute delayed VIBE sequences for all patients using image registration and analysis software (MIMVista Software) (see Fig. 1). PET and MR images were manually fused and registered together on the same software. ROIs were subsequently carried over from the MR to PET images to allow for measurements of activity and dose. Dose maps were created from the PET images by convolving the activity with a voxelized dose kernel, and dose volume histograms (DVHs) were calculated from these dose maps. Standardized uptake values (SUVs) were measured for each ROI, and ratios between tumor mean SUV and treated lobe mean SUV (tumor:treated), and treated lobe mean SUV and normal mean SUV (treated:normal) were calculated.

**RESULTS:** As shown in Table 1, of the 20 patients who underwent PET/MRI imaging, 100% of the patients had treated:normal SUV ratios >1 (Wilcoxon signed-rank test, $p<0.001$); 75% of the patients had tumor:treated SUV ratios ≥1; and 20% of the patients had a treated:tumor SUV ratio <1. Of the patients with hypervascular tumors—hepatocellular carcinoma (HCC) and neuroendocrine tumors (NET)—84.6% had tumor:treated SUV ratios ≥1. Of the patients with non-hypervascular tumors—colorectal cancer (CRC) and anal squamous cell carcinoma (AS)—57.1% had tumor:treated SUV ratios ≥1. Patients with the hypervascular tumors had higher tumor:treated SUV ratios than those with non-hypervascular tumors, though this did not reach statistical significance according to the Wilcoxon rank-sum test ($p=0.059$). There was a variety in $^{90}$Y uptake between patients, as illustrated in Fig. 1 (c, f).

**DISCUSSION:** The tumor:treated SUV ratios and DVHs demonstrate whether or not there is selectivity of $^{90}$Y delivering dose to the tumors as opposed the rest of the body and/or liver. Although most patients exhibited tumor:treated SUV ratios ≥1, there was still variability in the significance of this ratio between these patients, suggesting the need for post-procedural imaging. The greater uptake in the hypervascular tumors may suggest that these types of tumors may have a greater chance of responding to treatment; however, more follow-up imaging is required. While these measurements proved promising in allowing us to make delivery assessments using PET/MRI, there is still room for improvement, especially with motion correction. With the liver being in close proximity to the lungs and the long duration of the scans (~40 mins), both the MRI and PET images are highly susceptible to motion artifacts. Currently, we do not incorporate any motion correction into any of our scans, and manual registration of the two sequences is required in order to reduce misregistration error due to respiratory and other motion, although it does not eliminate it completely. Thus, incorporating motion correction algorithms into the experiment is essential for improving the accuracy of the treatment assessment metrics.

**CONCLUSION:** PET/MRI is feasible in assessing $^{90}$Y radioembolization for treatment of liver tumors. Future work will include improving image acquisition, especially in regards to motion correction, and incorporating follow-up imaging with tumor response.

| Tumor Type | Tumor Volume( cc) | Delivered Activity (GBq) | Treated: Normal SUV ratio | Tumor: Treated SUV ratio |
|---|---|---|---|---|
| **HCC** | 61.78 | 0.7 | 101:3.1 (33.1) | 308:101 (3.1) |
| | 1755.5 | 3.5 | 24.3:0.5 (45.4) | 26.6:24.3 (1.1) |
| | 5.0 | 1.03 | 60.0:3.2 (18.8) | 77.4:59.9 (1.3) |
| | 1514.3 | 2.99 | 61.3:1.2 (53.0) | 64.1:61.3 (1.1) |
| | 157.7 | 3.94 | 25.2:0.8 (31.7) | 77.6:25.2 (3.1) |
| | 185.0 | 2.21 | 73.6:0.6 (124.0) | 41.0:73.6 (0.6) |
| | 549.0 | 1.09 | 173.0:1.9 (89.7) | 173:173 (1.0) |
| **Ave** | **589.8** | | **56.5** | **1.6** |
| **NET** | 623.6 | 2.2 | 58.6:0.6 (94.3) | 100:58.6 (1.7) |
| | 55.5 | 1.5 | 64.3:0.9 (70.6) | 107:64.3 (1.7) |
| | NA* | 0.5 | 122:3.6 (34.3) | NA* |
| | 323 | 0.4 | 36.3:3.3 (11) | 55:36.3 (1.52) |
| | 21.0 | 0.4 | 32.8:0.8 (41.8) | 52:32.8 (1.6) |
| | 1170.0 | 5.8 | 22.6:0.8 (28.7) | 33.6:22.6 (1.5) |
| **Ave** | **439.5** | | **46.8** | **1.6** |
| **CRC** | 257.8 | 1.6 | 31:1.1 (28.9) | 30.4:31 (0.9) |
| | 2393.3 | 1.4 | 13.8:0.4 (37.6) | 10.4:13.8 (0.8) |
| | 212.1 | 0.9 | 50.7:4.0 (12.8) | 75.7:50.7 (1.5) |
| | 73.0 | 1.0 | 56.1:1.1 (49.5) | 30.3:56.1 (0.5) |
| | 122.1 | 1.3 | 33.9:5.6 (6.0) | 39.6:33.9 (1.2) |
| | 100.2 | 0.5 | 49.6:2.1 (23.6) | 47.3:49.6 (1.0) |
| **Ave** | **526.4** | | **26.4** | **0.9** |
| **AS** | 228.1 | 0.9 | 30.8:1.4 (22.2) | 69.3:30.8 (2.3) |
| **Total Ave** | **511.4** | | **42.5** | **1.5** |

**Table 1** Tumor demographics, delivered treatments and SUV values measured from PET data in patients who underwent $^{90}$Y radioembolization of the liver. HCC: hepatocellular carcinoma; NET: neuroendocrine tumors; CRC: colorectal cancer; AS: anal squamous cell carcinoma.

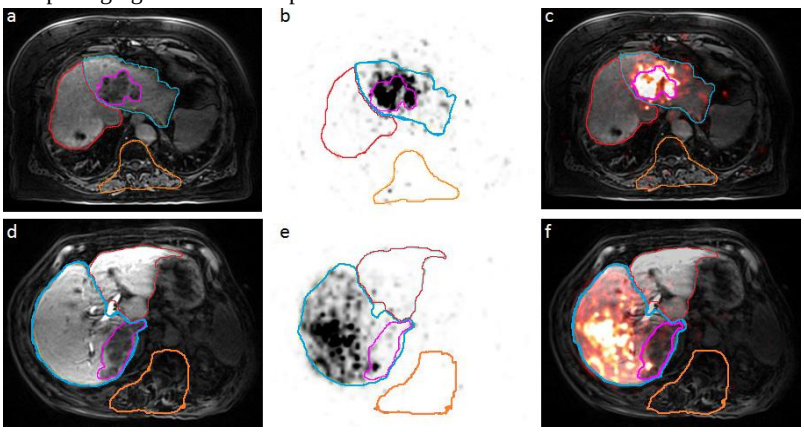


**Figure 1** MRI (a, d), PET (b, e), and fused PET/MRI (c, f) images of two patients who underwent $^{90}$Y radioembolization. Lesions (pink); treated lobe (blue); non-treated lobe (red); normal (orange). PET/MRI allows for simultaneous acquisition of both anatomical information (MRI) as well as localization information of $^{90}$Y activity (PET). The first patient (top) exhibits a liver that received most of its $^{90}$Y uptake within the tumor region (pink ROI). The second patient (bottom) exhibits a liver that did not receive most of its $^{90}$Y uptake within the tumor region (pink ROI), but rather in the rest of the treated side of the liver (blue ROI).